

Aspects of angle determination in coordinate metrology

Maryna Galovska¹, Michael Krystek^{2,*} and Reiner Tutsch¹

¹*Technische Universität Braunschweig, Institut für Produktionsmesstechnik, Schleinitzstraße 20, 38106 Braunschweig, Germany*

²*Physikalisch-Technische Bundesanstalt (PTB), Bundesallee 100, 38116, Braunschweig, Germany*

* *Corresponding author: michael.krystek@ptb.de*

Abstract

This work gives an overview of aspects of angle determination that is an important task of computational coordinate metrology. The algorithms of processing of point clouds for the estimation of angle between two planes and apex angle were analyzed. We studied the influence of sampling strategy on the variation of the angle estimates. An approach based on the fitting of combined geometries was proposed and its application to the angle determination task was demonstrated by the case study. document is a template for the online proceedings publication of the MacroScale conference.

1 Introduction

Coordinate metrology requires well-defined procedures for the determination of geometric primitives that allow unique parameterization of complex measurement objects and appropriate conformity assessment. Angle estimation is an important problem in areas of quality assurance, inspection planning, rapid prototyping, scene analysis for driver assistance systems, etc.

Development of the procedures for data processing collected by coordinate measurement systems is a task of computational coordinate metrology [1]. Different approaches to fit, filter and transform collected data can be applied taking into consideration the complexity of a measurement object and measurement strategy including the applied measurement instruments.

Extraction (ISO 14406:2010) based on the applied measurement strategy (discrete point, profile-based or area-based) provides input data that requires an appropriate 2D- or 3D-based algorithm. Area-based acquisition can be applied to measure features of objects from microscale to macroscale. Examples of the measurement objects, where the angle characterization is required, are given in Fig. 1. In this paper we discuss different aspects of the determination of: angle between two planes as parameter of their position with respect to each other (Chapter 2); apex angle as size parameter of a cone (Chapter 3) and angle from combined geometries (Chapter 4). The study of the influence of different sampling strategies and fitting algorithms on the angle estimate contributes to the computational coordinate metrology (Chapter 5).

Estimation of the angle from the measurement data obtained from instruments with area-based acquisition involves some typical problems of processing point clouds. Processing of point clouds includes: outlier detection (common for optical measurements), trimming, filtering and meshing. Important task-specific aspects are: decision about an outlier's removal, a choice of the filter and its cut-off, achieving a sufficient quality of the mesh. In this work we consider the aspects related to the angle estimation, especially fitting operation under the consideration of measurement uncertainty propagation.

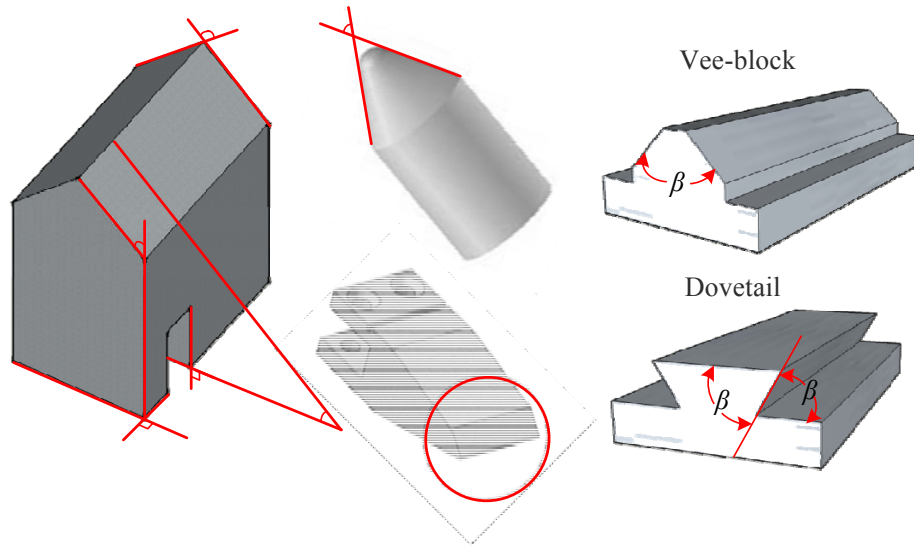


Figure 1: Example of the measurement objects from micro- to macroscale.

2 Estimation of the angle between two planes

Prism is an important geometry (see V-block and Dovetail profiles in Fig.1) formed by two intersecting planes and the angle between them, a parameter is included to GPS matrix [2]. The generalized scheme of angle estimation from a point cloud is given in Fig.2.

When measured points that belong to each of the plane cannot be easily separated, the partition has to be a part of the measurement strategy planning. Measurement of each plane might be performed in different measurement steps, by different measurement instruments and different measurement strategies. The common case of combined measurement with no obvious separating border between two planes requires partition (segmentation) of point clouds. An example of the partition is described in the Case Study (Chapter 6).

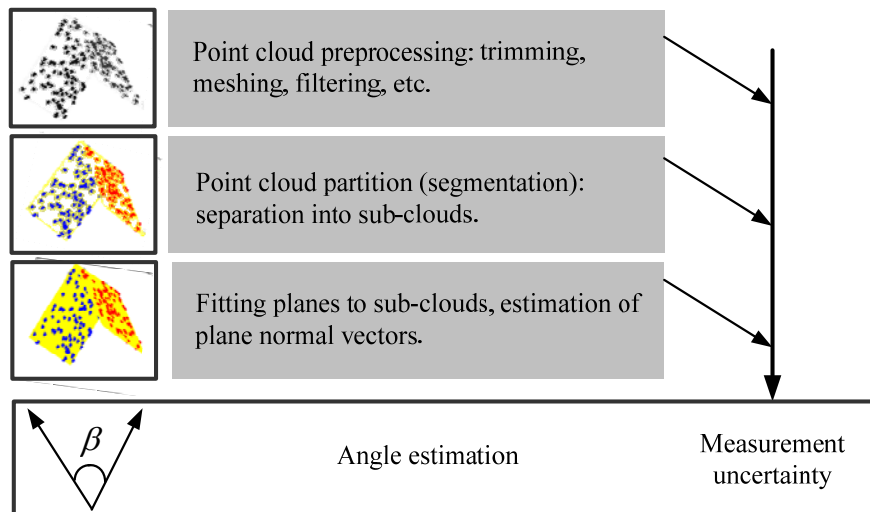


Figure 2: Generalized scheme of angle estimation from a point cloud

The core of the determination of the angle between two planes is the estimation of the normal vectors to the planes fitted to the sub-clouds (Fig.3).

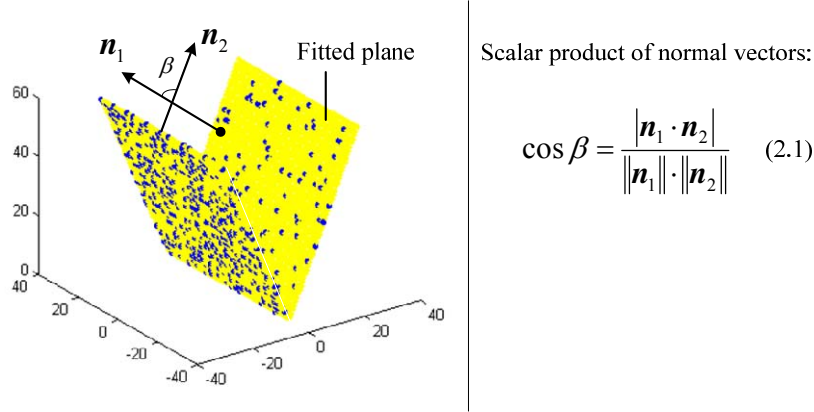


Figure 3: Plane fitting as the basis of angle estimation from a point cloud: \mathbf{n}_1 and \mathbf{n}_2 - normal vectors.

The basis of the association (ISO 17450-1:2011) is a fitting problem that can be solved using constrained or unconstrained optimization (minimization) of the objective function (2.2).

$$\Delta_n = \sum_{k=1}^N |d_k|^n, \quad (2.2)$$

where d - distance from data points to the profile surface of element; N – number of points; n – norm index.

Commonly used least-squares association (LS) is based on Gaussian norm ($n=2$):

$$\min \sum_{k=1}^N |d_k|^2 \quad (2.3)$$

LS-technique produces a stable best-fit surface and can be implemented based on eigenvector decomposition [3]. Parameters of a plane \mathbf{P} or normal vectors \mathbf{n}_i can be estimated as the eigenvector associated with the smallest eigenvalue of the matrix $\mathbf{A}^T \mathbf{A}$ that is formed for a point cloud $\mathbf{X} = (\mathbf{x}, \mathbf{y}, \mathbf{z})$ with the centroid $(\bar{x}, \bar{y}, \bar{z})$:

$$\mathbf{A} = \begin{pmatrix} \mathbf{x} - \bar{x} & \mathbf{y} - \bar{y} & \mathbf{z} - \bar{z} \\ \vdots & \vdots & \vdots \end{pmatrix}; \quad \text{eig}(\mathbf{A}^T \cdot \mathbf{A}) \Rightarrow \mathbf{P} \quad (2.4)$$

Realization of the minimum-zone fitting (MZ) base on Chebyshev norm ($n = \infty$) is more complicated. It is often used for the tasks of tolerance assignment. For example, parameters \mathbf{P} of MZ-plane can be estimated by linear programming for linear optimization problem with constraints:

$$\mathbf{A} = \begin{pmatrix} \mathbf{x} & \mathbf{y} & \mathbf{1} & \mathbf{1} \\ -\mathbf{x} & -\mathbf{y} & \mathbf{1} & -\mathbf{1} \end{pmatrix}; \mathbf{B} = \begin{pmatrix} \mathbf{z} \\ -\mathbf{z} \end{pmatrix}; \mathbf{C} = (\mathbf{0} \ \mathbf{0} \ \mathbf{0} \ \mathbf{1}); \quad \min \mathbf{C}^T \cdot \mathbf{P}, \text{ s.t.: } \mathbf{A} \cdot \mathbf{P} \leq \mathbf{B}; \quad \text{linprog}(\mathbf{C}, \mathbf{A}, \mathbf{B}) \Rightarrow \mathbf{P} \quad (2.5)$$

The efficiency of an angle estimator represents its uncertainty propagation. Comparison of estimators efficiency was carried out using Monte Carlo simulation. We simulated uncertainty of coordinates in a point cloud and compared distributions of obtained angle estimates (Fig.4). The variation of the angle estimate based on LS plane fitting (Fig.4, upper right) in the case of Gaussian distribution of the coordinates uncertainty is much lower compared to the variation of MZ-based estimate. Similarly, the point cloud can be accompanied with uniform distribution that gives similar values of variation for LS and MZ-based angle estimates (Fig.4, lower right).

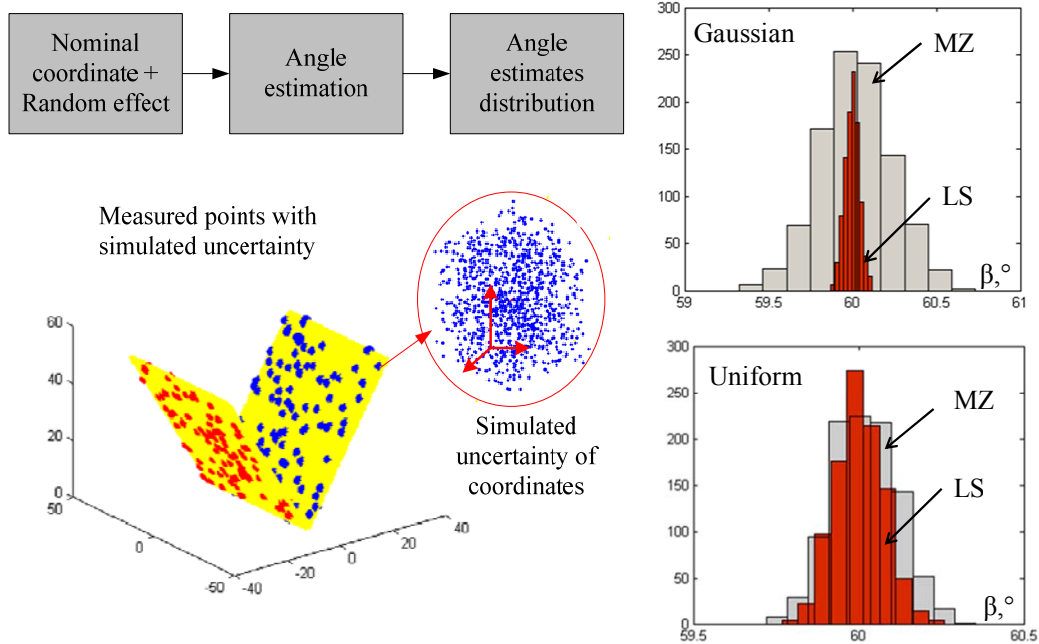


Figure 4: Study of the estimators efficiency: procedure of Monte Carlo simulation with 1000 iterations (left); distribution of angle estimates in cases of LSM and MZ plane fitting (right) for normal and uniform distribution of points coordinates.

3 Estimation of the angle between two planes

Cone (Fig. 5) is a geometry that belongs to the revolute class and its intrinsic characteristic according to ISO/TS 17450-1:2011 is the apex angle. According to the [3], a cone is specified by: a point on its axis (x_0, y_0, z_0) , a directional vector (a, b, c) along the axis and apex angle. Six parameters are estimated after minimization of sum of squares of distances from points to the cone under certain constraints ($c=1$). A Gauss-Newton algorithms from the library of the Least Squares Geometric Elements (LSGE) developed by NPL Centre for Mathematics and Scientific Computing (www.eurometros.org) was used as the reference to validate the results of angle estimation from Eq. 3.1-3.2.

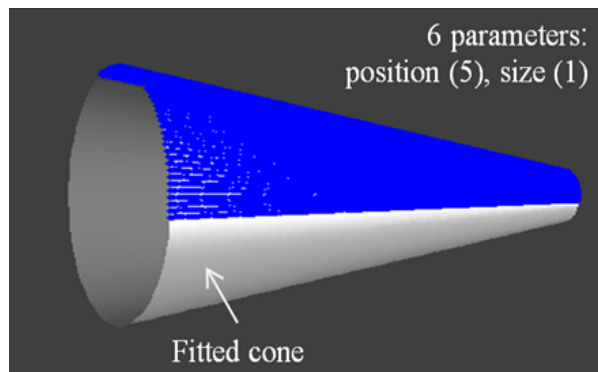


Figure 5: Cone fitting.

In terms of Euler angles, fitting of the cone to the point cloud requires an estimation of the apex angle β as the size parameter; two orientation parameters (φ, ψ) and three position parameters x_0, y_0, z_0 :

$$f = \mathbf{x}_{tr}^2 + \mathbf{y}_{tr}^2 - (z_{tr} \tan \beta)^2, \quad (3.1)$$

where the transformed coordinates are:

$$\begin{bmatrix} \mathbf{x}_{tr} \\ \mathbf{y}_{tr} \\ \mathbf{z}_{tr} \end{bmatrix} = R_{tr}(\varphi, \psi) \begin{bmatrix} \mathbf{x} - \mathbf{x}_0 \\ \mathbf{y} - \mathbf{y}_0 \\ \mathbf{z} - \mathbf{z}_0 \end{bmatrix}, \quad (3.2)$$

$$R_{tr}(\varphi, \psi) = R_{tr}(\varphi) \cdot R_{tr}(\psi) = \begin{bmatrix} 1 & 0 & 0 \\ 0 & \cos(\varphi) & -\sin(\varphi) \\ 0 & \sin(\varphi) & \cos(\varphi) \end{bmatrix} \cdot \begin{bmatrix} \cos(\psi) & 0 & \sin(\psi) \\ 0 & 1 & 0 \\ -\sin(\psi) & 0 & \cos(\psi) \end{bmatrix}.$$

The solutions for a non-linear objective function are found by either approximating the objective function or using iterative techniques. Commonly used algorithms are: Steepest Descent, Gauss-Newton and Levenberg-Marquardt. The function (Eq.3.1-3.2) were used to estimate β using a solver for non-linear optimization.

4 Estimation of angle as a part of combined geometry

Complex shapes include combination of different geometric primitives. Combined geometries can be used to fit the model of the object without a directly applied *partition*. This approach requires the complete mathematical model associated with the measurement object. An association in this case is denoted by a complex objective function and its constraints. In Fig. 6(a) a geometric model and simulated point clouds corresponding to the *combined geometric elements* are presented. A decomposition of the object (Fig. 6(b)) yields a sphere and a cone. The object shown in Fig. 6(c) consists of a cylinder and two tangential planes. The two main geometric parameters that describe the sizes of the objects are: radius of the cylinder or sphere (r) and the angle between the planes or the apex angle of the cone (β). These parameters define the unique relative position of the geometric primitives. We proposed the models for the association of combined geometry [4].

The point T (Fig. 6(a)) that separates the geometric primitives has the coordinate:

$$y_T = r \cdot (\cos(\beta/2))^2 / \sin(\beta/2), \quad (4.1)$$

A combination of a cone and a sphere in Fig. 6(b) is described by the following model, which incorporates both size parameters (r, β). It is used for the association of the complete point cloud with the substitute geometry:

$$\begin{cases} f(1) = \mathbf{x}_{tr}^2 + \mathbf{y}_{tr}^2 + (z_{tr} \tan(\beta/2))^2, & \mathbf{y}_{tr} > y_T \\ f(2) = \mathbf{x}_{tr}^2 + \mathbf{y}_{tr}^2 + (z_{tr} - r / \sin(\beta/2))^2 - r^2, & \mathbf{y}_{tr} < y_T \end{cases} \quad (4.2)$$

Similarly, the following objective function can be used for the combination of a cylinder and two planes as represented in Fig. 6(c):

$$\begin{cases} f(1) = (\mathbf{y}_{tr} - \cot(\beta/2) \cdot |\mathbf{x}_{tr}|)^2, & \mathbf{y}_{tr} > y_T \\ f(2) = \mathbf{x}_{tr}^2 + (\mathbf{y}_{tr} - r / \sin(\beta/2))^2 - r^2, & \mathbf{y}_{tr} < y_T \end{cases} \quad (4.3)$$

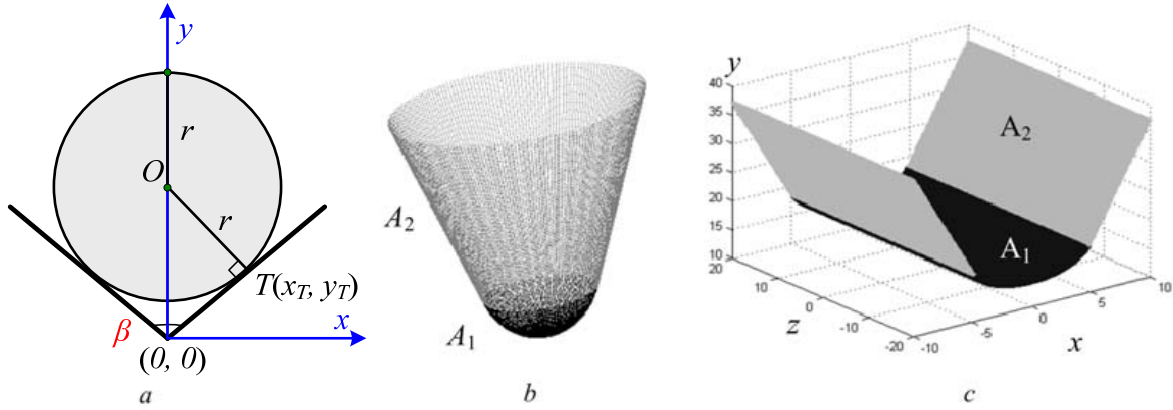


Figure 6: Basic models for association including partition: 2D model (a); 3D models (b, c).

The Rotation matrix includes three rotation angles and Eq.(3.2) can be extended by the third term:

$$R_r(\varphi, \psi, \theta) = R_r(\varphi, \psi) \cdot \begin{bmatrix} \cos(\theta) & -\sin(\theta) & 0 \\ \sin(\theta) & \cos(\theta) & 0 \\ 0 & 0 & 1 \end{bmatrix}.$$

The optimization problem is carried out to evaluate the unknown parameters including the angle β from the point cloud. Sometimes an unconstrained optimization shows a poor convergence. In this case additional boundary conditions are useful [4].

5 Influence of sampling strategy

Sampling strategy that includes the number, location and distribution of the measured points has a strong influence on the angle estimate for any estimation method described above. The number of points has an obvious influence on the variation of the estimate: higher number of points leads to decreasing the variation. In this work the location/distribution of measured points is studied. Monte Carlo simulation and *resampling* were used as the basis for the study.

The following routine was used for the study:

- (1) Two planes simulated without form deviations ($\beta = \pi/3$).
- (2) Iteratively repeated (number of iterations 5000): random extraction of points from the initial sets (resampling) correspondent to each of the planes; adding a random component (Gaussian distribution with zero mean and standard deviation $SD = 0.2 \text{ mm}$) to each coordinate; angle estimation based on LS plane.
- (3) Statistical analysis of obtained angle estimates.

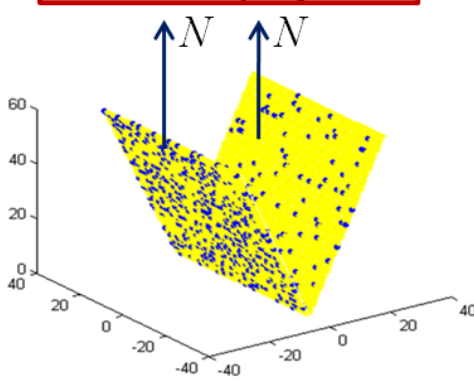
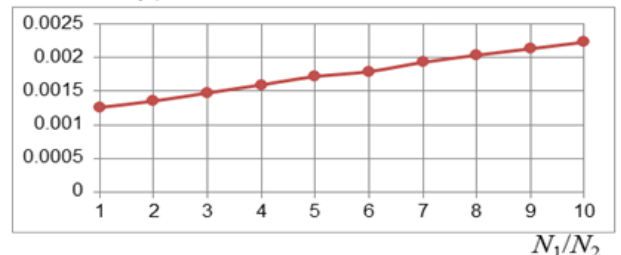
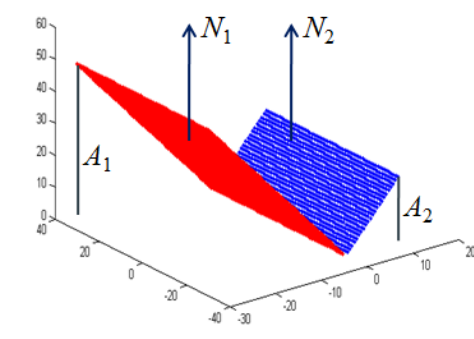
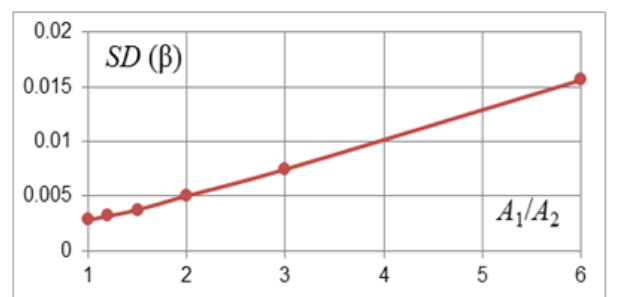
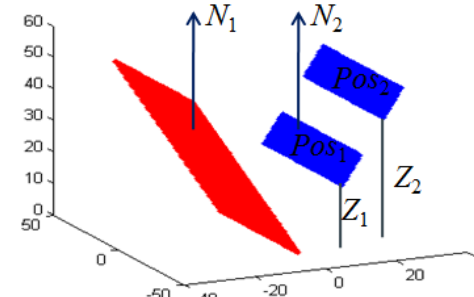
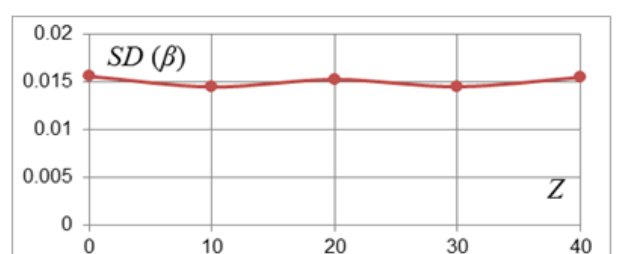
In Table 1 the simulation strategies and their results are given. The results of the study are represented in form of standard deviations for the angle estimates depending on the value of variation parameter. By changing of the ratio of the number of points that belong to each of the planes N_1/N_2 , we studied the influence of the point density on the angle estimate.

For the second study the number of points was kept constant, but the size of the acquisition area (area covered by measured points) was changing. Obviously, a higher ratio of acquisition areas A_1/A_2 causes a higher uncertainty of the angle estimates.

The position of one acquisition area in respect to the other (in a case of negligible form deviations of the plane) showed no significant influence on the result of the angle evaluation.

An important conclusion from the study: the uncertainty of the angle estimate strongly depends on the "symmetry" of the sampling strategy. The results can to be taken into account for the measurement strategy planning, particularly for the position of the measurement object position or, in case of the optical techniques, the position of measurement cameras.

Table 1: Study of sampling strategy.

Simulation illustration	Results of simulation																						
1. Influence of point density on the uncertainty of angle estimate																							
<p style="border: 1px solid red; padding: 2px; display: inline-block;">Resampling $N_1 + N_2 = 1000$</p> 	<p>Ratio of number of points N_1/N_2 that belong to each of the planes is variable.</p> <p>$SD(\beta)$</p>  <table border="1" style="display: none;"> <caption>Data for SD(beta) vs N1/N2</caption> <thead> <tr> <th>N_1/N_2</th> <th>$SD(\beta)$</th> </tr> </thead> <tbody> <tr><td>1</td><td>0.0012</td></tr> <tr><td>2</td><td>0.0013</td></tr> <tr><td>3</td><td>0.0014</td></tr> <tr><td>4</td><td>0.0015</td></tr> <tr><td>5</td><td>0.0016</td></tr> <tr><td>6</td><td>0.0017</td></tr> <tr><td>7</td><td>0.0018</td></tr> <tr><td>8</td><td>0.0019</td></tr> <tr><td>9</td><td>0.0020</td></tr> <tr><td>10</td><td>0.0021</td></tr> </tbody> </table>	N_1/N_2	$SD(\beta)$	1	0.0012	2	0.0013	3	0.0014	4	0.0015	5	0.0016	6	0.0017	7	0.0018	8	0.0019	9	0.0020	10	0.0021
N_1/N_2	$SD(\beta)$																						
1	0.0012																						
2	0.0013																						
3	0.0014																						
4	0.0015																						
5	0.0016																						
6	0.0017																						
7	0.0018																						
8	0.0019																						
9	0.0020																						
10	0.0021																						
2. Influence of sizes of acquisition areas on the uncertainty of angle estimate																							
<p style="border: 1px solid red; padding: 2px; display: inline-block;">Resampling $N_1 = N_2 = 100$</p> 	<p>Acquisition area of the second plane A_2 is variable.</p> <p>$SD(\beta)$</p>  <table border="1" style="display: none;"> <caption>Data for SD(beta) vs A1/A2</caption> <thead> <tr> <th>A_1/A_2</th> <th>$SD(\beta)$</th> </tr> </thead> <tbody> <tr><td>1</td><td>0.003</td></tr> <tr><td>2</td><td>0.005</td></tr> <tr><td>3</td><td>0.008</td></tr> <tr><td>4</td><td>0.010</td></tr> <tr><td>5</td><td>0.013</td></tr> <tr><td>6</td><td>0.016</td></tr> </tbody> </table>	A_1/A_2	$SD(\beta)$	1	0.003	2	0.005	3	0.008	4	0.010	5	0.013	6	0.016								
A_1/A_2	$SD(\beta)$																						
1	0.003																						
2	0.005																						
3	0.008																						
4	0.010																						
5	0.013																						
6	0.016																						
3. Influence of location of measured points on the uncertainty of angle estimate																							
<p style="border: 1px solid red; padding: 2px; display: inline-block;">Resampling $N_1 = N_2 = 100$</p> 	<p>Position of the second covered area (Pos_2) is variable.</p> <p>$SD(\beta)$</p>  <table border="1" style="display: none;"> <caption>Data for SD(beta) vs Z</caption> <thead> <tr> <th>Z</th> <th>$SD(\beta)$</th> </tr> </thead> <tbody> <tr><td>0</td><td>0.015</td></tr> <tr><td>10</td><td>0.014</td></tr> <tr><td>20</td><td>0.015</td></tr> <tr><td>30</td><td>0.014</td></tr> <tr><td>40</td><td>0.015</td></tr> </tbody> </table>	Z	$SD(\beta)$	0	0.015	10	0.014	20	0.015	30	0.014	40	0.015										
Z	$SD(\beta)$																						
0	0.015																						
10	0.014																						
20	0.015																						
30	0.014																						
40	0.015																						

6 Case study

The approaches of angle estimates were tested for the measured data (from ATOS system of GOM company). A measured point cloud that is a part of a complex geometry demonstrates the described aspects of angle determination (Fig. 7). The conventional approach requires the partition of the point cloud into sub-clouds of points that correspond to each of two planes. Different approaches to the segmentation of data could be used: clustering, Hough transformation, RANSAC or curvature based approach.

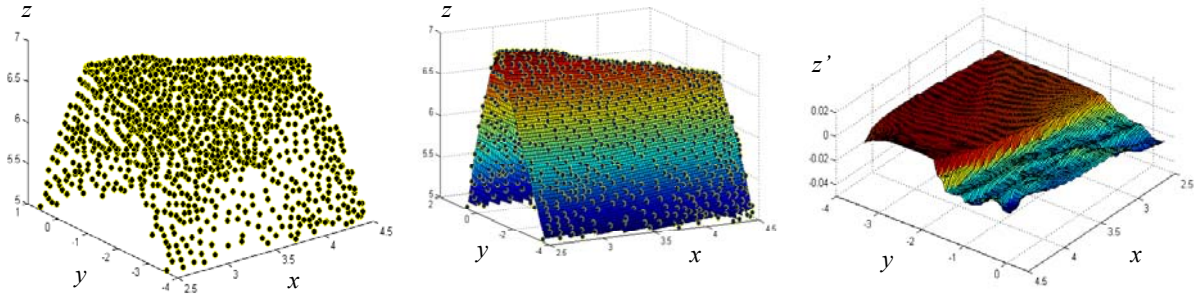


Figure 7: Measured by ATOS point cloud (left), derived surface (middle) and its gradient (right).

We use gradient (second derivative) to separate sub-clouds. For this purpose, first a regular grid was obtained from the scattered points. Its gradient demonstrates differences between two planes: one of the sides contains significant form deviations caused by manufacturing (laser sintering). Otsu's method was used to threshold and separate the sub-clouds by gradient values. The form deviations on the side and on the edge are a source of the partition error shown in Fig. 8.

The partition error is the source of the bias in the angle estimate. The estimate based on MZ plane (see Table 2) is extremely sensitive to this error, whereas the LS-based estimate is more robust. The difference between estimates constitutes about 10° .

To exclude the influence of the partition error the sub-clouds were trimmed (the points of the upper part of the scan were not included to the estimation). In this case, the difference between LS-based and MZ-based estimates is much lower (about 1°). The trimming of the point clouds means losing data that is not desirable. We used the developed approach (Chapter 4) taking into account a rounding between flat areas. The model according to Eq. 4.3 was used to estimate the angle. We obtained the plausible value of the angle estimate 87.73° and the radius estimate 0.19 mm.

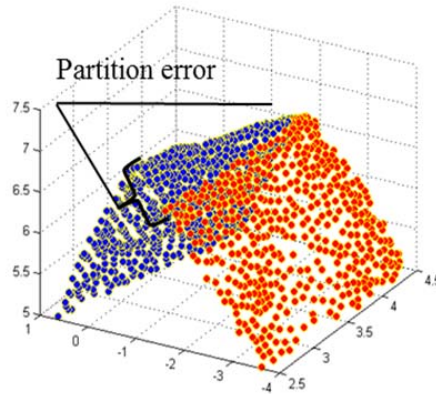


Figure 7: Results of partition.

Table 2: Study of sampling strategy.

	Sub-clouds with partition error	Trimmed sub-clouds	Complete point cloud
LS	87.88°	87.63°	87.73°
MZ	77.78°	88.66°	-

7 Conclusion

Different aspects of the determination of the angle between two planes and apex angle of cones were shown. We described a procedure of point cloud processing to obtain a reliable angle estimate and proposed approaches for its improvement.

Starting from the measurement strategy development, the location and distribution of measurement points have to be taken into account. A combination of Monte Carlo method and resampling technique was used for the sampling strategy study.

A typical problem of point cloud processing is the geometry partition or segmentation. The errors of partitions leads to the deviation of the angle estimate. This was demonstrated by the case study. The way to avoid them based on the fitting of combined geometric elements was proposed.

References

- [1] Srinivasan V 2012 Reflections on the Role of Science in the evolution of dimensioning and tolerancing standards *Proc IMechE Part B: J Engineering Manufacture* **227(1)** 3–1.
- [2] ISO 2538:1998 Geometrical Product Specifications (GPS) - Series of angles and slopes on prisms.
- [3] Forbes A B 1991 NPL Report DITC 140/89: Least-squares best-fit geometric elements, National Physical Laboratory, Teddington, UK.
- [4] Galovska M, Krystek M and Tutsch R 2014 Curvature radii characterization based on point clouds. *Technisches Messen*: **81** 39-47.